Improving the energy conversion efficiency of a laser-driven flyer by an in-situ fabricated nano-absorption layer

Liang Wang
University of Electronic Science and Technology of China
Yichao Yan
University of Electronic Science and Technology of China
Xiangbo Ji
Institute of Chemical Materials
Wanli Zhang
University of Electronic Science and Technology of China
Hongchuan Jiang
University of Electronic Science and Technology of China
Wenzhi Qin
Institute of Chemical Materials
Yao Wang
Institute of Chemical Materials
Duo Tang (Kristanson_tang@caep.cn)
Institute of Chemical Materials https://orcid.org/0000-0003-4662-8058

Nano Express

Keywords: Laser-driven flyer, Nanostructured absorption layer, Energy conversion, PDV

Posted Date: April 13th, 2020

DOI: https://doi.org/10.21203/rs.3.rs-16710/v2

Version of Record: A version of this preprint was published at Nanoscale Research Letters on June 5th, 2020. See the published version at https://doi.org/10.1186/s11671-020-03346-5.

Abstract

Three kinds of Al flyer plates with different nanostructured absorption layers were in-situ prepared by a direct laser writing technology to improve the energy conversion efficiency in a laser-driven flyer assembly. Microstructures, light absorption, flyer velocity in the acceleration chamber were investigated. The reflectance for the flyers at 1064 nm wavelength can be reduced from 81.3% to 9.8% by the nanostructured absorption layer. The terminal velocity of a 50 μm thick Al flyer irradiated by a 60mJ laser pulse is 831 m/s, while the velocity of the flyer with an in-situ fabricated nano-absorption layer reaches up to 1113 m/s at the same condition. Resultantly, the energy conversion efficiency of the flyer with nanostructure absorption layer can reach as high as 1.99 times that of the Al flyer. Therefore, the nanostructured absorption layer in-situ prepared on the surface of a flyer provides a new method to significantly improve the energy conversion efficiency of a laser-driven flyer.

1. Introduction

Laser-driven flyer (LDF) used for detonating explosives offers a promising approach to well controlled, short-pulse shock compression of condensed phase materials [1-4]. In a LDF setup, a thin metal foil supported by a transparent window substrate is often launched by a nanosecond pulsed laser, a layer of the metal foil named ablation layer is ablated generating high pressure plasmas instantly, the plasmas then drive the remains of the metal foil to fly at a velocity of several km/s as a flyer. Metal aluminum is ideal as the flyer material due to its good tenacity and low density. However, since a large fraction of energy is lost due to high reflection of the pure aluminum flyer, the energy conversion efficiency of the flyer (defined as the ratio between the flyer kinetic energy and the incident laser energy) is extremely low, which has greatly limited the practical applications of the LDF [5-6].

Plenty of works have been carried out for the purpose to improve the energy conversion efficiency of LDF. Considering the energy conversion efficiency could be improved by introducing a layer with stronger absorption at the incident laser wavelength due to decreased reflection [7], many materials with lower reflectivity compared to pure aluminum have been studied as the absorption layer. Labaste [8] and Brierley [9] investigated several materials as absorption layer to improve the energy conversion efficiency, and found that the addition of Ge, Ti and Zn can decrease the reflection and slightly increase the flyer velocity. A single coat of black paint has also been applied as the absorption layer of the flyer, but the velocity was not obviously improved. Since these low reflective materials serve not only as absorption but also ablation layer, while the interaction material efficiency depends on both the optical and the thermodynamic properties of the flyer material [10], the increase of flyer velocity is limited.

Recently, the use of plasmonic nanomaterials to improve the light absorption through an excitation of localized surface plasmon resonance (LSPR) has attracted considerable interest in the fields of spectroscopic sensors and solar energy conversion [11-13]. Aluminum nanostructures can be used as light-harvesting systems because it covers up a wide spectrum range from ultraviolet to visible light of LSPR [14-17]. Zhang [18] found that an enhancement of 40% in absorption could be achieved by

integrating the aluminum particles by using optical simulations. Lee [19] reported a design strategy to achieve a robust platform for plasmon-enhanced light harvesting using aluminum core-shell nanostructures, which resulted in a remarkable increase in photo-to-chemical conversion. Fan [20] demonstrated an ultrafast laser processing strategy for fabricating highly effective antireflection micro-nano structures on thick metal surfaces, and an average reflectance of 4.1%, 2.4%, and 3.2% in the broadband spectrum from ultraviolet to near-infrared on Cu, Ti, and W surfaces were achieved. However, to our best knowledge, there is no research on using nanostructured material to improve the laser absorption in LDFs.

In this work, we propose a nanostructured aluminum absorption layer in-situ prepared on the surface of thin Al flyers to improve the laser absorption and energy conversion efficiency. A femtosecond laser writing technology named as direct laser writing was utilized to fabricated the nanostructures due to its precision, relative simplicity, and high yielding rate [21-23]. The morphology and composition of the surface of the in-situ prepared nanostructures were characterized and their light absorption was tested. To evaluate the energy conversion efficiency of the flyers with a nanostructured absorption layer, the flyers were launched using single pulsed lasers and their velocities were obtained by a Photonic Doppler Velocimetry (PDV). Furthermore, the kinetic energy and energy conversion efficiency of the flyers were calculated and discussed.

2. Experimental Methods

2.1 Sample preparation

Al foils with 60mm×60mm×50μm (width, length and height) were used as the reference flyer. These foils were first electric-chemical polished to achieve a low surface average roughness. The nanostructured absorption layers were then in-situ prepared on the surface of Al foils by a direct writing laser under an air atmosphere. The direct laser writing used a polarized femtosecond laser (FX200-3-GFH, EdgeWave, Germany) with a wavelength of 1030nm, pulse duration of 600fs, and repetition rate of 200kHz. The output laser power varied from 0W to 100 W. Fig. 1 illustrates the direct laser writing preparation process to fabricate the samples. The nanostructures on the surface of Al foils were controlled by changing the radiation laser power, scanning speed and period. Three samples with different nanostructured absorption layers (Sample A, B, and C) were prepared. Sample A was irradiated by 22.60W laser pulses with 1000mm/s scanning speed in y direction and 25μm scanning period. Sample B was irradiated by 13.82W laser pulses with 5000mm/s scanning speed in both x and y directions and 1μm scanning period. Sample C was irradiated by 22.60W laser pulses with 8000mm/s scanning speed in both x and y directions and 100nm scanning period.

2.2 Characterization methods

The morphology of the surface of the samples was characterized by scanning electron microscopy (SEM，Ultra 55, Zeiss, Germany) combined with energy dispersive X-ray analysis (EDX, Oxford, Britain). The optical wavelength-dependent reflectivity measurement in the wavelength from 500nm to 1500nm

for the samples were carried out with an UV-VIS-NIR spectrophotometer (SolidSpec-3700, Shimadzu, Japan) incorporated with an integrating sphere.

Fig. 2 illustrates the experimental setups used to launch the flyer and characterize the flyer velocity as the velocity is one of the key factors to estimate the flyer performance. A Q-switched Nd:YAG laser (Innolas SpitLight 400, 1064nm wavelength, 14ns pulse length) was employed to ablate and launch the prepared samples, and a PDV system is applied to measure the flyer velocity of the samples. The spatial energy distribution of the laser beam was homogenized by a diffusive optic, since the focused beam itself was highly non-uniform. The laser spot had a diameter of 0.5mm. In the velocimetry experiment, samples were cut into small pieces and adhered onto a sapphire window with the nanostructured layer clung to the window. Steel acceleration chambers with a thickness of 0.2mm and an inner diameter of 0.6mm were used. 60mJ single laser pulses were shot on the samples to produce fast flying flyers in the acceleration chamber. An optical fiber connected with the PDV system was placed at the exit of the acceleration chamber to record the velocity of the flyer.

3. Results And Discussion

3.1 Microstructure of the absorption layer

Fig. 3(a-f) shows the microstructure of the nanostructured absorption layer of Sample A, B and C, respectively. Since Sample A was irradiated by ultrafast lasers in one direction with a scanning speed of v_x=0 and v_y=1000mm/s, the surface of sample A exhibits semi-periodic structures, as shown in Fig.3a. A nano-spherical structure was observed for Sample A in Fig. 3d. The nano-spheres with about 50-200nm diameter were covered with smaller nano-spheres whose diameters were less than 10 nm. Sample B and C were irradiated in both directions and their scanning speed are much higher than Sample A, no evident periodic structures were observed on their surfaces, as shown in Fig. 3b and Fig. 3c. As for Sample B, many particles in the scale of micrometers were observed on its surface(Fig. 3b), and the particles were composed of cauliflower nanostructures(Fig. 3e). Since Sample C were irradiated and scanned by an even higher speed compared with Sample A and B, the accumulation of nanoparticles was much faster and the heat effect were more prominent. Consequently, much thicker nanosheet and nanoparticle aggregations were observed in Fig. 3c and Fig. 3f. And multiple cracks occurred on the surface because relatively high stress was emerged during the cooling process due to prominent heat input.

Fig. 3(g-i) are the energy dispersive X-ray analysis (EDX) results for Sample A, B and C, respectively. The EDX showed the presence of Al_2O_3 oxides in the composition of nanostructures. The oxides were formed due to the oxidation of aluminum during laser writing process. The oxygen contents of Sample A, B and C were 2.2, 8.4 and 22.9 atom%, respectively. Apparently, Sample B and C had much higher oxygen content compared to Sample A, while the irradiation laser power for Sample B(13.82W) was lower than that of Sample A(22.60W) and the irradiation laser power for Sample A and C were identical, indicating that the scanning speed and scanning period significantly influence the heat generation and dissipation during

direct laser writing. And the oxidation increases with the increase of scanning speed and decrease of the scanning period.

3.2 Light absorption of the samples

Fig. 4 a shows the optical microscope appearances of Al foil and the flyers with nanostructured absorption layer. The color of Al foil is silvery white. With the addition of nanostructured absorption layer, Sample A, B and C exhibits grey, black and dark black colors, indicating that more light can be absorbed with the absorption layer. The reflectance of Al foil and Sample A, B and C is tested by a spectrophotometer, and the measurements is repeated two times for each sample. Fig. 4b shows the reflectance spectrum of Al foil and the aluminum flyer with nanostructure absorption layer. Since the transmitting thickness of infrared light through metals often varies from a few tens of nanometers to several hundreds nanometers [24], thus none of the light was transmitted through the Al foil samples whose thickness were 50μm. And the scattered light was included in the reflected light in the measurement using an integral sphere. Consequently, the absorption could be calculated by 1-R(reflectance). Differences were evident between Al foil and the aluminum flyer with nanostructured absorption layer. The reflectance of Al foil was 81.3% at the laser wavelength of 1064 nm, indicating that 81.3% of incidence light was reflected. The average reflectance can be reduced to 50.5%, 31.5%, and 9.8% for Samples A, B and C, respectively. Therefore, light absorption can be effectively enhanced with the nanostructure absorption layer prepared by direct laser writing. Sample C has the strongest absorption (90.2%) at 1064nm compared to Sample A and B. Aside from the effect of the nanostructures, we believe that the aluminum oxide presented in the nanostructures also tremendously influences the light absorption of the flyer. Generally, Al_2O_3 is transparent and doesn't absorb light, however, in a direct laser writing process, it is highly possible for the generated Al_2O_3 and aluminum particles to form a metal-dielectric-metal structure. The structure behaves as an F-P cavity which will in turn enhance the surface plasmon resonance and increase the light absorption [25]. As the oxygen concentrations of Sample A and B are far less than that of Sample C, implicating that the Al_2O_3 particles is richer in Sample C than other samples, resultantly, a more enhanced surface plasmon resonance effect and far stronger absorption can be achieved.

3.3 Velocity of the flyer

Fig. 5 shows the flyer velocities of Al foil, Sample A, B and C. At the beginning of 30 ns, the flyer velocity increases sharply. Afterward, the flyer velocity gradually increases starting from 30 ns to 200 ns, and hardly changes when the time exceeds 200 ns. The terminal flyer velocity for Sample A, B and C is 1083m/s, 1173m/s and 1110m/s, respectively, which is about 1.30, 1.41, and 1.33 times higher than that of the Al foil (831m/s). These results confirmed that the addition of an in-situ nanostructured layer can not only enhance the light absorption but also promote the flyer velocity. It's worth mentioning that the flyer velocity for Sample B is higher than Sample C whilst Sample C has the strongest light absorption. The reason is that Sample C has a far richer Al_2O_3 content compared with Sample B. Ionic bond and metal bond was formed in Al_2O_3 and Al, respectively. And it was known that ionic bond was far stronger

than metal bond, which makes the vaporization point and melting point for Al_2O_3 higher than Al. The melting point and vaporization point for Al_2O_3 is 2054℃ and 2980℃, while the melting point and vaporization point for Al is 660℃ and 2519℃, respectively. Additionally, the thermal conductivity is 29.3W/m·K and 237W/m·K for Al_2O_3 and Al. Hence, it is more difficult for Al_2O_3 to vaporize and form plasma at the incident pulsed laser due to its high melting point and low thermal conductivity compared to pure aluminum [26]. Therefore, although the light absorption is enhanced by Al_2O_3 in Sample C, in the meantime, Al_2O_3 consumes some of the incident laser energy while it doesn't help driving the flyer.

The kinetic energy of the flyers can be obtained by the following relationship.

[Please see the supplementary files section to view the equation.] (1)

Where m_f is the original flyer mass; m_a represents the ablated flyer mass. Moreover, we assume the flyer keeps an integrated state during the flying process. The ablated flyer mass can be evaluated according to Lawrence and Trott model [27].

[Please see the supplementary files section to view the equation.] (2)

Where r is the radius of the flyer; μ_{eff} is the effective absorption index; I_0 is the incident laser intensity; k is the energy loss index; ε_d is the vaporization energy.

The energy conversion efficiency of the flyer can be denoted using the following equation.

[Please see the supplementary files section to view the equation.] (3)

The calculated results of the flyer kinetic energy and energy conversion efficiency were illustrated in Fig. 6. The energy conversion efficiency for Sample A, B and C is 36.8%, 43.2% and 38.6%, which is 1.70, 1.99 and 1.78 times that of the Al foil(21.7%). In this work, when a nanostructured absorption layer is added on Al foil, the highest energy conversion efficiency almost doubled. The experimental results are summarized in Table 1. Therefore, the in-situ fabrication of a nanostructured absorption layer on the surface of a flyer provides a new method to significantly improve the energy conversion efficiency of a LDF.

4. Conclusions

Nanostructured absorption layers were successfully in-situ prepared on the surface of thin Al foils by direct laser writing technology. Furthermore, we demonstrated that through controlling the laser pulse injection, both the microscale and nanoscale structural features can be realized. Consequently, a substantial decrease in light reflectivity and a significant enhancement in light absorption can be realized. By in-situ preparing the nano-absorption layer on the surface of an Al foil, the light absorption can be increased from 18.7% to 90.2%. The increase in light absorption will in turn result in an evident increase in the velocity and kinetic energy of a laser driven flyer. The energy conversion of the flyer with

nanostructured absorption layer can be significantly improved compared with Al foil, the max energy conversion in this study reaches up to 43.2% which is 1.99 times that of the Al foil(21.7%). Therefore, the aluminum nanostructure absorption layer in-situ prepared on the surface of the flyer provides a new method to increase the absorption of laser energy and improve the energy conversion efficiency of a LDF. Moreover, the in-situ preparation technology present in this work is also promising in fields of photochemistry, sensing, photodetectors and quantum optics.

Declarations

Availability of data and materials

All authors declare that the materials, data, and associated protocols are available to the readers, and all the data used for the analysis are included in this article.

Competing interests

The authors declare that they have no competing interests.

Funding

This work was supported by the Natural Science Foundation of China (No. 11902305).

Authors' contributions

LW carried out the experimental work and characterization measurement and wrote the paper. YCY and XBJ assisted in the measurement and data analysis. WLZ made corrections to the manuscript. WZQ and YW assisted in the measurement. HCJ and DT made instructions and supervised the whole work. All authors read and approved the final manuscript.

Acknowledgements

We sincerely thank Prof. Wei Xiong at the Huazhong University of Science and Technology for the support in sample preparation.

Authors' information

Not applicable

References

1. Guo W, Wu LZ, He NB, Chen SJ, Zhang W, Shen RQ, Ye YH. Efficiency relationship between initiation of HNS-IV and nanosecond pulsed laser-driven flyer plates of layered structure. Laser and Particle Beams. 2018; 36: 29-40.

2. Watson S, Gifford MJ, Field JE. The initiation of fine grain pentaerythritol tetranitrate by laser-driven flyer plates. Journal of Applied Physics. 2000; 88:65-69.
3. Brown KE, Shaw WL, Zheng X, Dlott DD. Simplified laser-driven flyer plates for shock compression science. Review of Scientific Instruments. 2012; 83:103901.
4. Dean SW, De Lucia FC, Gottfried JL. Indirect ignition of energetic materials with laser-driven flyer plates. Applied Optics. 2017; 56: B134-B141.
5. Sallé B, Chaléard C, Detalle V, Lacour JL, Mauchien P, Nouvellon C. Laser ablation efficiency of metal samples with UV laser nanosecond pulses. Applied Surface Science. 1999; 138(139): 302-305.
6. Guo W, Wu LZ, Meng NX, Chen YR, Ma ZP, Zhou X, Zhang W, Shen RQ, Ye YH. Optimisation of modulation period of TiO_2/aluminum reactive multilayer films for laser-driven flyer plates. Chemical Engineering Journal. 2019; 360:1071-1081.
7. Zhang HN, Wu LZ, Hu P, Guo W, Zhang W, Ye YH, Shen RQ. Launch and impact characteristics of typical multi-layered flyers driven by ns-pulsed laser. Optics & Laser Technology. 2019; 120:1-10.
8. Labaste JL, Brisset D, Doucet M. Investigation of driving plasma materials for laser acceleration of flyer plates. AIP Conference Proceedings. 2000; 505:1189-92.
9. Brierley HR, Williamson DM, Vine TA. Improving laser-driven flyer efficiency with high absorptance layers. AIP Conf. Proc. 2012; 1426:315-318.
10. Yu H, Fedotov V, Baek W, Yoh JJ. Towards controlled flyer acceleration by a laser-driven mini flyer. Applied Physics A: Materials Science & Processing. 2014; 115:971–978.
11. Wang Y, Zhai J, Song YL. Plasmonic cooperation effect of metal nanomaterials at Au-TiO2-Ag interface to enhance photovoltaic performance for dye-sensitized solar cells. RSC Advances. 2015; 5:210-214.
12. Zhao Y, Hoivik N, Akram MN, Wang KY. Study of plasmonics induced optical absorption enhancement of Au embedded in titanium dioxide nanohole arrays. Optical Materials Express. 2017; 7: 2871-2879.
13. Guo SH, Li XH, Ren XG, Yang L, Zhu JM, Wei BQ. Optical and electrical enhancement of hydrogen evolution by MoS_2@MoO_3 core-shell nanowires with designed tunable plasmon resonance. Advanced Functional Materials. 2018; 28:
14. Katyal J, Soni RK. Size- and shape-dependent plasmonic properties of aluminum nanoparticles for nanosensing applications. Journal of Modern Optics. 2013; 60:1717-1728.
15. Ren Y, Hu SY, Ji BY, Zou P, Liu LW, Li Y. Fano resonance in aluminum nano-dolmen plasmonic structure for enhanced biosensing. Sensing and Bio-Sensing Research. 2017; 15:5-11.
16. Zhang FF, Martin J, Plain J. Long-term stability of plasmonic resonances sustained by evaporated aluminum nanostructures. Optical Materials Express. 2019; 9:85-94.
17. Smith KJ, Cheng Y, Arinze ES, Kim NE, Bragg AE, Thon SM. Dynamics of energy transfer in large plasmonic aluminum nanoparticles. ACS Photonics. 2018; 5: 805-813.

18. Zhang DB, Yang XF, Hong XK, Liu YS, Feng JF. Aluminum nanoparticles enhanced light absorption in silicon solar cell by surface plasmon resonance. Optical and Quantum Electronics. 2015; 47:1421-1427.
19. Lee M, Kim JU, Lee KJ, Ahn S, Shin YB, Shin J, Park CB. Aluminum nanoarrays for plasmon-enhanced light harvesting. ACS Nano. 2015; 9:6206-6213.
20. Fan PX, Bai BF, Zhong ML, Zhang HJ, Long JY, Han JP, Wang WQ, Jin GF. General Strategy Toward Dual-Scale-Controlled Metallic Micro-Nano Hybrid Structures with Ultralow Reflectance. ACS Nano. 2017; 11:7401-7408.
21. Wei Y, Chen J, Song XF, Gu Y, Zeng HB. Laser direct-writing electrode for rapid customization of a photodetector. Optics Letters. 2019; 44:683-687.
22. Lamont AC, Alsharhan AT, Sochol RD. Geometric determinants of in-situ direct laser writing. Scientific Reports. 2019; 9:394.
23. Tong QC, Luong MH, Remmel J, Do MT, Nguyen DTT, Lai ND. Rapid direct laser writing of desired plasmonic nanostructures. Optics Letters. 2017; 42:2382-2385.
24. Wang SX, Zhang ZG, Yin C. The Influence of Absorption Layer Thickness On Dynamic Responses of the Laser Shocked Metal. Material Engineering and Mechanical Engineering: Proceedings of Material Engineering and Mechanical Engineering. 2015.
25. Zhao R, Zhai T, Wang Z, Liu D. Simultaneous excitation of cavity resonance and surface plasmon resonance in Ag/Al2O3/Ag layer structure. Appl Phys B. 2008; 92:585-588.
26. Bowden MD, Knowles SL. Optimisation of laser-driven flyer velocity using Photonic Doppler velocimetry. Optical technologies for arming, safing, fuzing and firing, San Diego: CA, 2009, 7434: 1-11.
27. Lawrence RJ, Trott WM. Theoretical analysis of a pulsed-laser-driven hypervelocity flyer launcher. International Journal of Impact Engineering. 1993; 14:439-449.

Table

Table. 1 Summarization of the experimental results

Sample	Laser energy (mJ)	Reflectance	Velocity(m/s)	Kinetic energy(mJ)	Conversion efficiency
Al foil	60	81.3%	831	13.0	21.7%
Sample A		50.5%	1083	22.1	36.8%
Sample B		31.5%	1173	25.7	43.2%
Sample C		9.8%	1110	23.0	38.6%

Figures

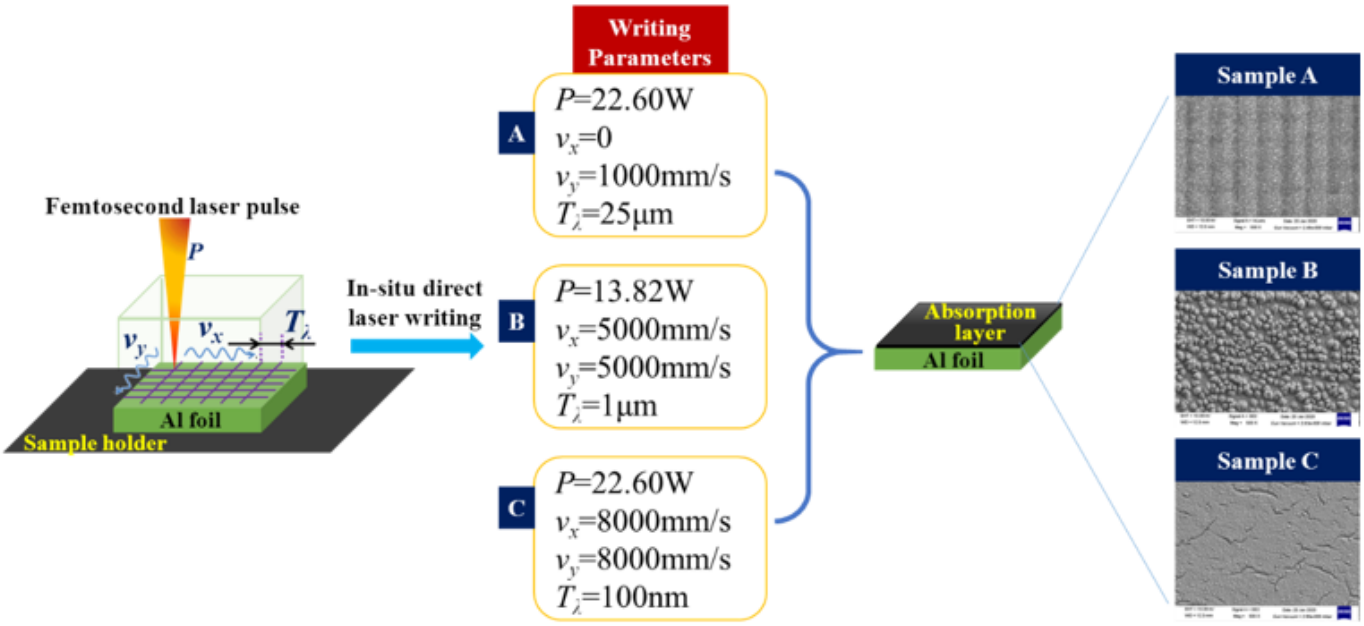

Figure 1

Schematics of the sample preparation method.

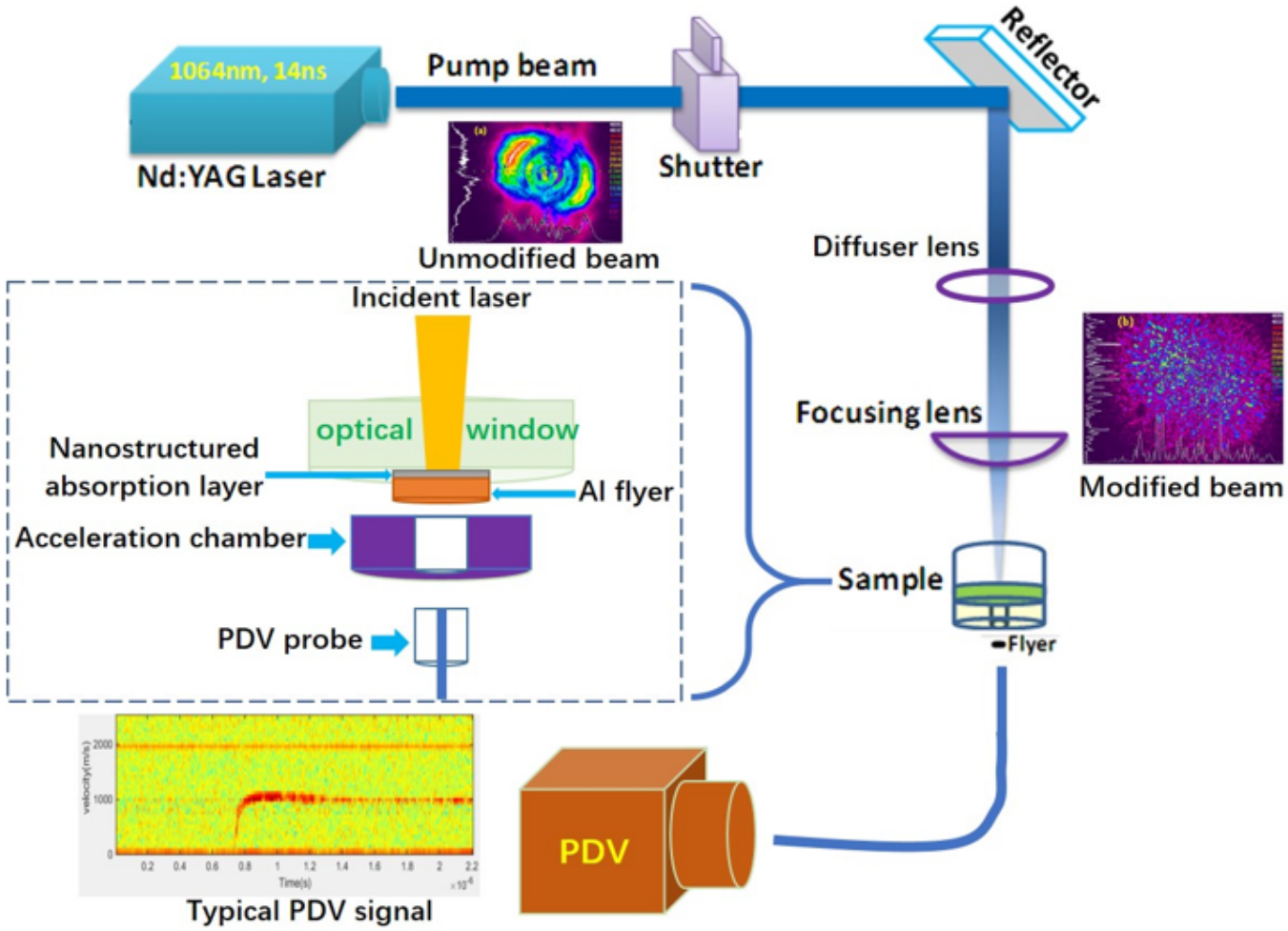

Figure 2

Schematics of the flyer launching system and flyer velocity recording system (PDV).

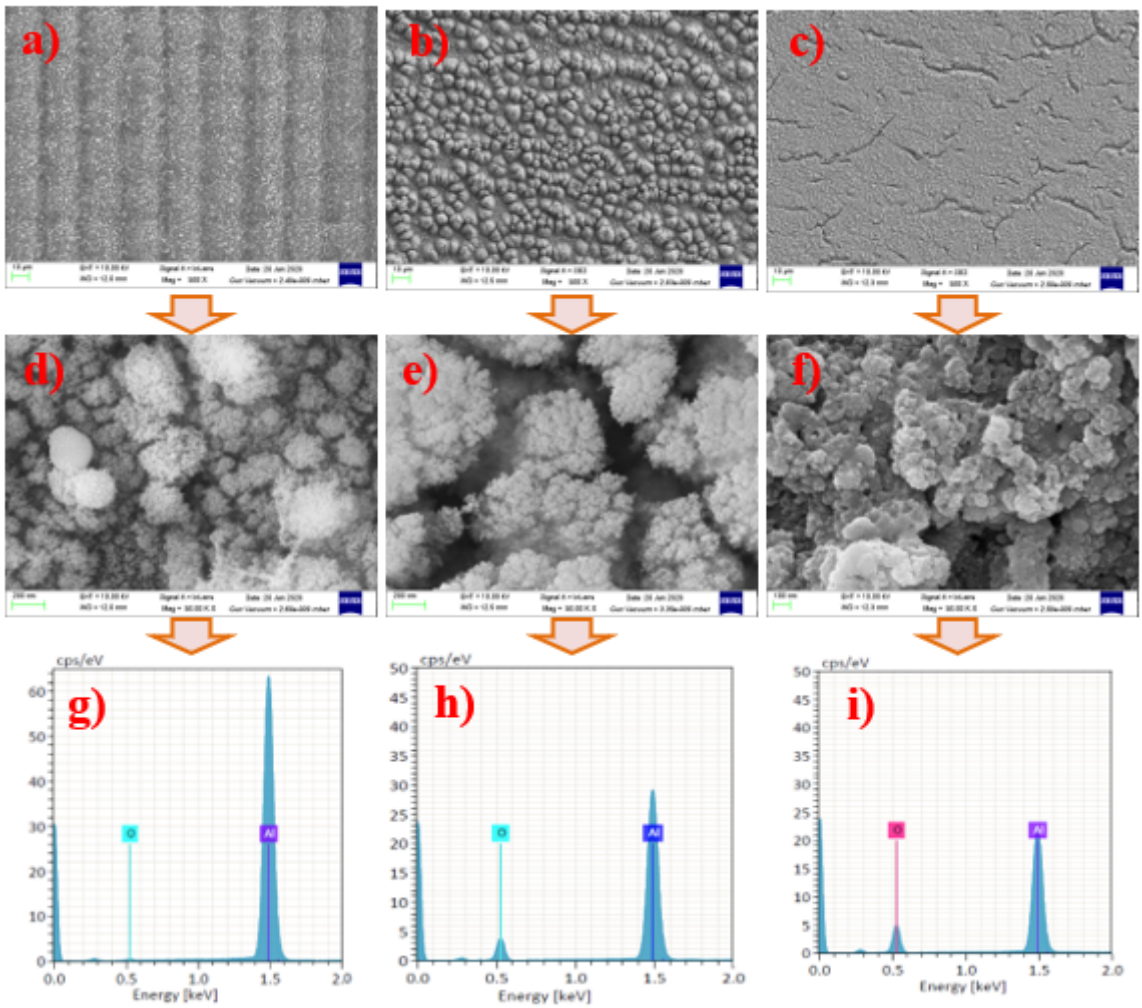

Figure 3

a SEM images with 1000X magnified for Sample A. b SEM images with 1000X magnified for Sample B. c SEM images with 1000X magnified for Sample C. d SEM images with 4000X magnified for Sample A. e SEM images with 4000X magnified for Sample B. f SEM images with 4000X magnified for Sample C. g EDX for Sample A. h EDX for Sample B. i EDX for Sample C.

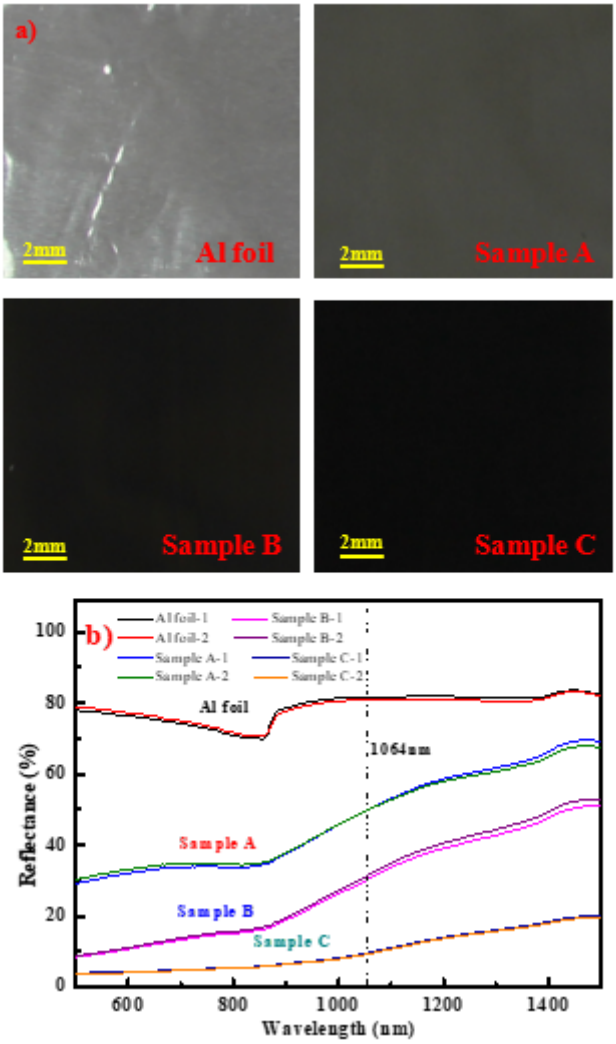

Figure 4

a Optical microscope appearances of Al foil, Sample A, B and C. b The reflectance spectrum of Al foil, Sample A, B and C.

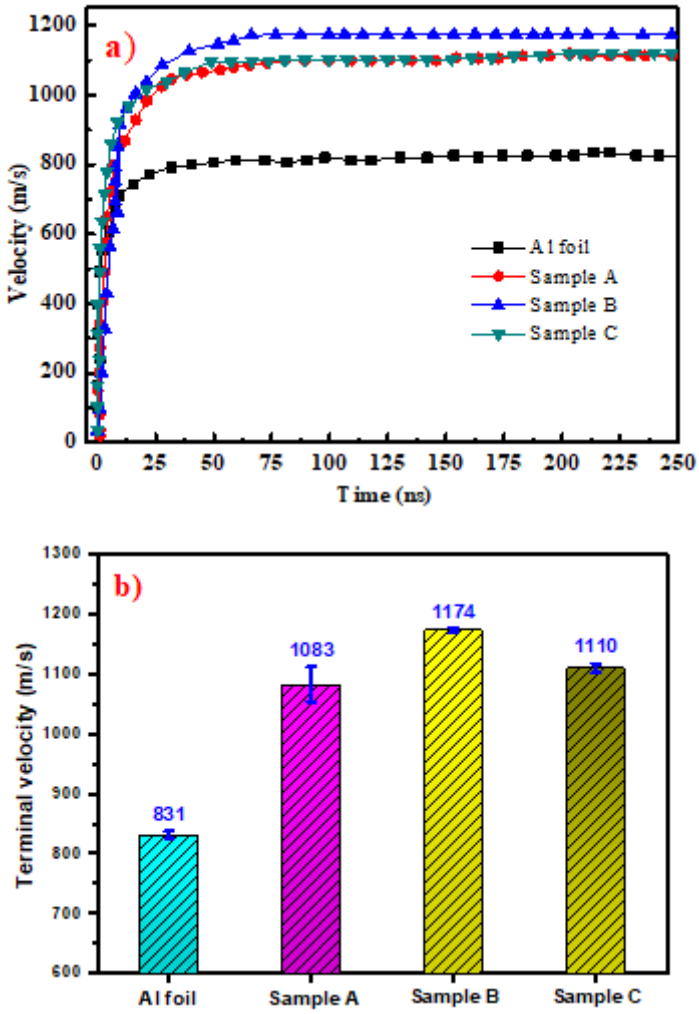

Figure 5

a The flyer velocities of Al foil and Sample A, B and C in the acceleration chamber obtained using PDV. b The terminal flyer velocities of Al foil and Sample A, B and C.

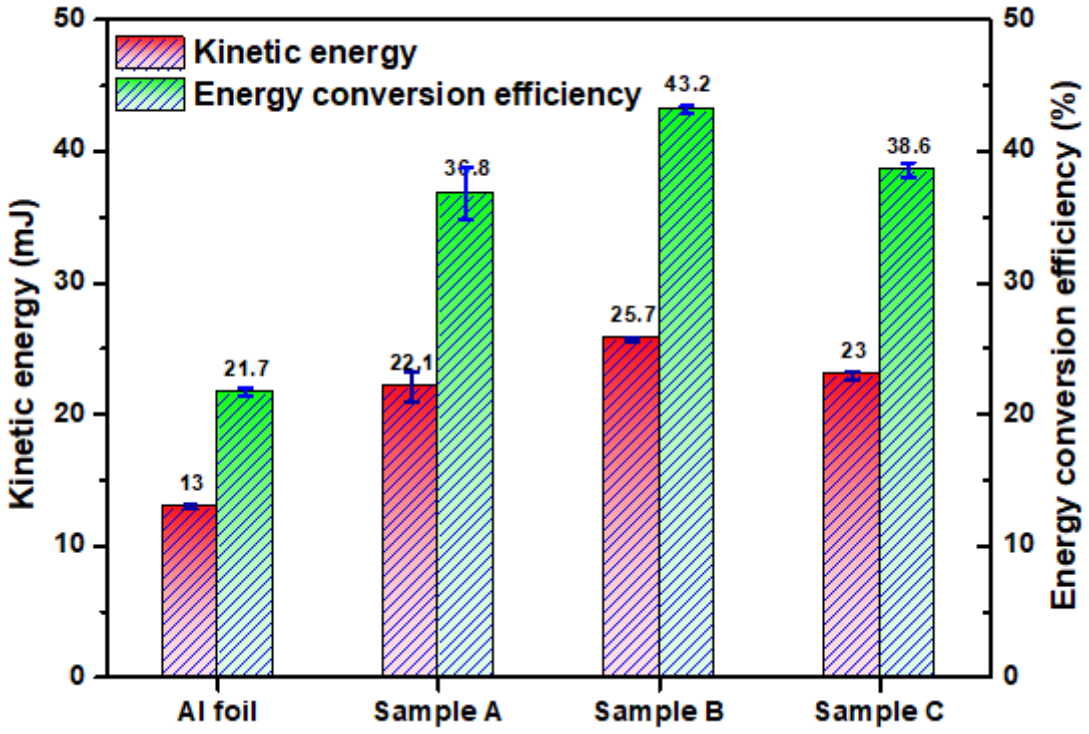

Figure 6

The calculated kinetic energy and energy conversion efficiency of Al foil and Sample A, B and C.

Supplementary Files

This is a list of supplementary files associated with this preprint. Click to download.

- Equations.docx
- Supplement.docx